GEOPHYSICAL RESEARCH LETTERS, VOL. 34, L05501, doi:10.1029/2006GL028737, 2007

Near zero replenishment of the Arctic multiyear sea ice cover at the end of 2005 summer

Ron Kwok[1]

Received 10 November 2006; revised 9 January 2007; accepted 25 January 2007; published 2 March 2007.

[1] The remarkably low Arctic multiyear (MY) sea ice coverage following the summer of 2005 is placed in the context of its variability over the past seven years (2000–2006). Annual cycles of MY ice coverage, from QuikSCAT and satellite passive ice motion, show that the replenishment of MY ice area at the end of this summer is near zero (0.1×10^6 km^2) compared to the previous five summers of 1.0, 1.2, 0.4, 0.4, and 0.9×10^6 km^2. This is examined in terms of anomalies in ice export and the record of freezing (F_{DD}) and melting degree-days (M_{DD}). The 2005 summer (Jun–Sep) saw the highest Fram Strait ice export (>0.25×10^6 km^2) compared to the 7-year mean of 0.14×10^6 km^2. This directly explains ~40% of the decrease in MY coverage of 0.6×10^6 km^2 between Jan 2005 and Jan 2006. The cumulative effects of the recent warmer winters and summers, relative to the longer-term record since 1958, explain the balance. For this short record, the combination of spatially averaged F_{DD} and M_{DD} anomalies of the preceding year explain ~63% of the variance in the replenishment areas. **Citation:** Kwok, R.2007), Near zero replenishment of the Arctic multiyear sea ice cover at the end of 2005 summer, *Geophys. Res. Lett.*, *34*, L05501, doi:10.1029/2006GL028737.

1. Introduction

[2] At the end of every Arctic summer, seasonal ice thick enough to survive the melt season is classified as multiyear (MY) ice. This ice replenishes the reservoir of MY ice that was depleted by ice export or summer melt. Multiyear ice is thicker than first-year ice because of its greater age and thus more growth by freezing; this old ice allows the existence of a large summer ice cover that is unique to the Arctic. Reduction in MY replenishment and coverage could be due to increased melt during the summer and ice export through Fram Strait or other passages. Persistent decreases in the summer ice coverage would lead to increases in summer heating of the ocean and decreases in the ice volume of the Fram Strait outflow - a major source of surface fresh water for the Greenland-Iceland-Norwegian Seas.

[3] Over the passive microwave satellite record, negative trends of ~7–10% per decade in the Arctic Ocean MY sea ice cover have been estimated by *Johannessen et al.* [1999] and more recently by *Comiso* [2002, 2006]. This rate of decline can be compared to the more moderate rate of −3% per decade in the total sea ice extent of the Northern Hemisphere. A recent analysis by *Nghiem et al.* [2006] reports a remarkable decrease in multiyear ice extent (~0.7×10^6 km^2) in 2005 when compared with the coverage in 2004; with the largest decrease in the Eastern Arctic. The winter MY coverage of the Arctic Ocean in 2006 stands at ~50% compared to that of ~70% two decades ago.

[4] While there are now reasonable estimates of the recent decline in MY coverage of the Arctic Ocean, the variability in the MY ice replenishment area at the end of summer has not been estimated. This key parameter is the area of first-year (FY) ice that survives the summer and relates directly to ice export, summer melt, and the thickness of the ice cover at the beginning of the melt season. Higher summer melt, higher ice export, and thinner ice all contribute to the lowering of the replenishment area. The present note examines this replenishment area, A_r, with annual cycles of MY coverage constructed using 7-year records (2000–2006) of QuikSCAT MY analysis and Fram Strait ice flux from satellite passive microwave observations. The dependence of A_r on the record of freezing and melting temperatures of the preceding winter and summer is explored. The contribution of summer ice export and melt to the large decline in MY coverage between 2005 and 2004 is estimated.

2. Data Description

[5] The data sets used in this work include: (1) ice export and ice concentration estimates from satellite passive microwave data; (2) MY fraction derived from QuikSCAT; and (3) daily sea level pressure and temperature fields from the NCEP-NCAR analysis products [*Kalnay et al.*, 1996].

[6] Export of MY ice at the Fram Strait is estimated using the procedure described by *Kwok and Rothrock* [1999] and *Kwok et al.* [2004]. The primary flux gate is located roughly parallel to 81°N and spans the ~400 km width between Antarctic Bay in northeast Greenland and the northwestern tip of Svalbard. It is positioned as far north as possible to obtain the best estimate of Arctic Ocean ice area export. Farther south, area changes due to ice melt and divergence are likely and thus less representative of the outflow. Winter ice area flux (October through May) is computed from daily ice motion derived from the 85 GHz channel of the SSM/I brightness temperature fields by integrating the gate-perpendicular component of the motion profile between the two coastal endpoints. The motion profile is weighted by satellite ice concentration and MY ice concentration, and is constrained to go to zero at these endpoints. The expected monthly uncertainty in area flux during the winter is ~6.0×10^3 km^2.

[7] As motion estimates are unreliable during the summer months, the monthly area export (F_{summer}) is estimated

[1]Jet Propulsion Laboratory, California Institute of Technology, Pasadena, California, USA.

0094-8276/07/2006GL028737$05.00

using the following relationship between monthly ice flux and sea-level pressure gradient across the Strait [*Kwok et al.*, 2004]:

$$F_{summer} = 5.9\Delta P + 78.7 \quad \left(10^3\ \mathrm{km}^2\right).$$

ΔP (in hPa) is the mean monthly cross-strait pressure gradient and explains more than 70% of the variance in ice area export. This relationship is derived from a 22-year record of ice export and ΔP. This area flux is weighted by ice concentration. Monthly flux uncertainty is higher in the summer and is estimated at $\sim 7.5 \times 10^3$ km^2.

[8] The seven years of winter MY ice coverage of the Arctic is from QuikSCAT (launched in 1999) backscatter fields [*Kwok*, 2004]. The maps of MY fraction on January 1 and April 30 of each the seven winters are shown in Figures 1d and 1e. The backscatter contrast between MY and FY ice is used for obtaining these estimates. Details of this procedure and its relative merits compared to the passive microwave approach can be found in the work of *Kwok* [2004] and *Kwok et al.* [1999]. Uncertainties in coverage are $\sim 150 \times 10^3$ km^2.

3. Analysis and Discussion

3.1. Annual Cycles of Multiyear Ice Coverage (2000–2006)

[9] Here, we provide only a brief description of the procedure used to construct annual cycles of MY sea ice coverage of the Arctic Ocean [*Kwok*, 2004]. As the MY ice coverage, A_{MY}, is not directly observable in QuikSCAT data in all seasons, the time series shown in Figure 2 is obtained by considering the area balance of MY ice within the Arctic Ocean over annual cycles between October and September. Using the fact that ice export explains a large fraction of the Arctic MY ice coverage, we can write:

$$A_{\mathrm{MY}}(t) = A_{\mathrm{MY}}(Jan-1) - \left(A_{\mathrm{MY-export}}(t) - A_{\mathrm{MY-export}}(Jan-1)\right). \quad (1)$$

The annual cycle begins on October 1 (i.e., $t = 0$) near the beginning of the growth season. We use the QuikSCAT MY coverage on the first of each calendar year (i.e., $A_{\mathrm{MY}}(Jan\text{-}1)$) to provide an area tie-point because the reliability of this estimate is highest in the middle of winter. At the beginning of freeze up, the signatures of MY and FY ice are unstable due to moisture on the surface [*Kwok*, 2004]. In equation (1), $A_{\mathrm{MY\text{-}export}}(t)$ is the time-series of cumulative MY ice area export at the Fram Strait and other passages (sign is positive for export). This construction of $A_{\mathrm{MY}}(t)$ assumes that MY sea ice does not melt and deforms little. During the winter (Oct–May), these are reasonable statements. Also, we assume that lateral melt of thick MY year ice during the summer is negligible. Even though this could be an issue as the MY ice cover thins, the area balance results provide an upper bound estimate of summer (Jun–Sep) Arctic MY ice coverage. The root-sum-squared of the uncertainties in monthly export ($\sim 7 \times 10^3$ km^2) and MY coverage from QuikSCAT ($\sim 150 \times 10^3$ km^2) provide an estimate of the expected uncertainty in the MY coverage time series (error bars in Figure 2).

[10] The annual cycles of A_{MY} (in Figure 2) show a monotonic decrease in coverage from the beginning of the growth season that is due to ice flux primarily through Fram Strait: $\sim$10% of the Arctic Ocean ice cover is lost to export every year. Ice export is typically lower during the summer months (Jun–Sep) because of reduced ΔP and lower MY fraction at the flux gate. The step increase in MY ice area at the end of each summer is the FY ice area that survives the summer. These FY ice areas replenish the MY ice reservoir after each year's depletion through export and melt. A balance between export and replenishment is necessary to maintain a stable MY ice cover. For the six summers from 2000 to 2005, these areas are: 1.0, 1.2, 0.4, 0.4, 0.9, and 0.1×10^6 km^2. The variability is remarkably high. The near zero replenishment at the end of summer of 2005, at 0.1×10^6 km^2, stands out as the smallest of the six summers. Because of this low replenishment, the MY ice coverage in January 2006 is lower by $\sim 0.6 \times 10^6$ km^2 when compared to that in January 2005 and is the lowest over the record. The next sections examine this abrupt decline in terms of the anomalies in ice export within the longer-term record of freeze and melt over the Arctic Ocean.

3.2. Large Export During the Summer of 2005

[11] Ice export is typically lower during the summer months (Jun–Sep) because of reduced wind forcing and lower MY fraction at the flux gate. The summer ice export for the seven years (2000–2006) ranges between 0.1×10^6 km^2 (in 2002) and 0.25×10^6 km^2 (in 2005), with a mean of 0.15×10^6 km^2 and standard deviation of 0.05×10^6 km^2. The anomalously high summer export in 2005, at $>1.5\sigma$ from the mean, is due to the Fram Strait outflow in August and September. This can be seen in the normalized monthly anomalies in pressure gradient ($\Delta\tilde{P} = \frac{\Delta P - \Delta\bar{P}}{\sigma_{\Delta P}}$) across the Fram Strait (Figure 1c) during these two months. $\Delta\bar{P}$ and $\sigma_{\Delta P}$ are the 7-year monthly means and standard deviations. The $\Delta\tilde{P}$ of these two months in 2005, at $\sim$2 and $\sim$2.5, represent large deviations from the norm, thus forcing large areas of sea ice through the Fram Strait. This can be compared to the much smaller $\Delta\tilde{P}$ of other summers.

[12] On an Arctic Ocean scale, these anomalously high gradients are associated with the patterns of sea level pressure (SLP) distributions shown in Figure 3. In the mean August and September SLP fields, the high density of isobars perpendicular to the Fram Strait is evident. These gradients are associated with troughs of low pressure in the Greenland Sea in August and in Barents/Norwegian Seas in September. Since ice motion is largely wind-driven and nearly parallel to the isobars of surface pressure, the result is an increased sea ice outflow. In particular, the arrangement of SLP pattern in September also shows a strong Transpolar drift stream that favors the Eastern Arctic Ocean as the source region of sea ice exported through Fram Strait. This suggests that the large depletion of the MY ice cover in the Eastern Arctic reported by *Nghiem et al.* [2006] can in part be explained by the anomalous SLP patterns during the summer. This large expanse of first-year ice in the Eastern Arctic on January 2006 can be seen Figures 1d and 1e.

[13] The consequence of summer ice export is different from that of the winter. During the winter or growth season, the MY ice depleted by area export is replaced by FY ice. Depending on the winter conditions, these seasonal ice areas

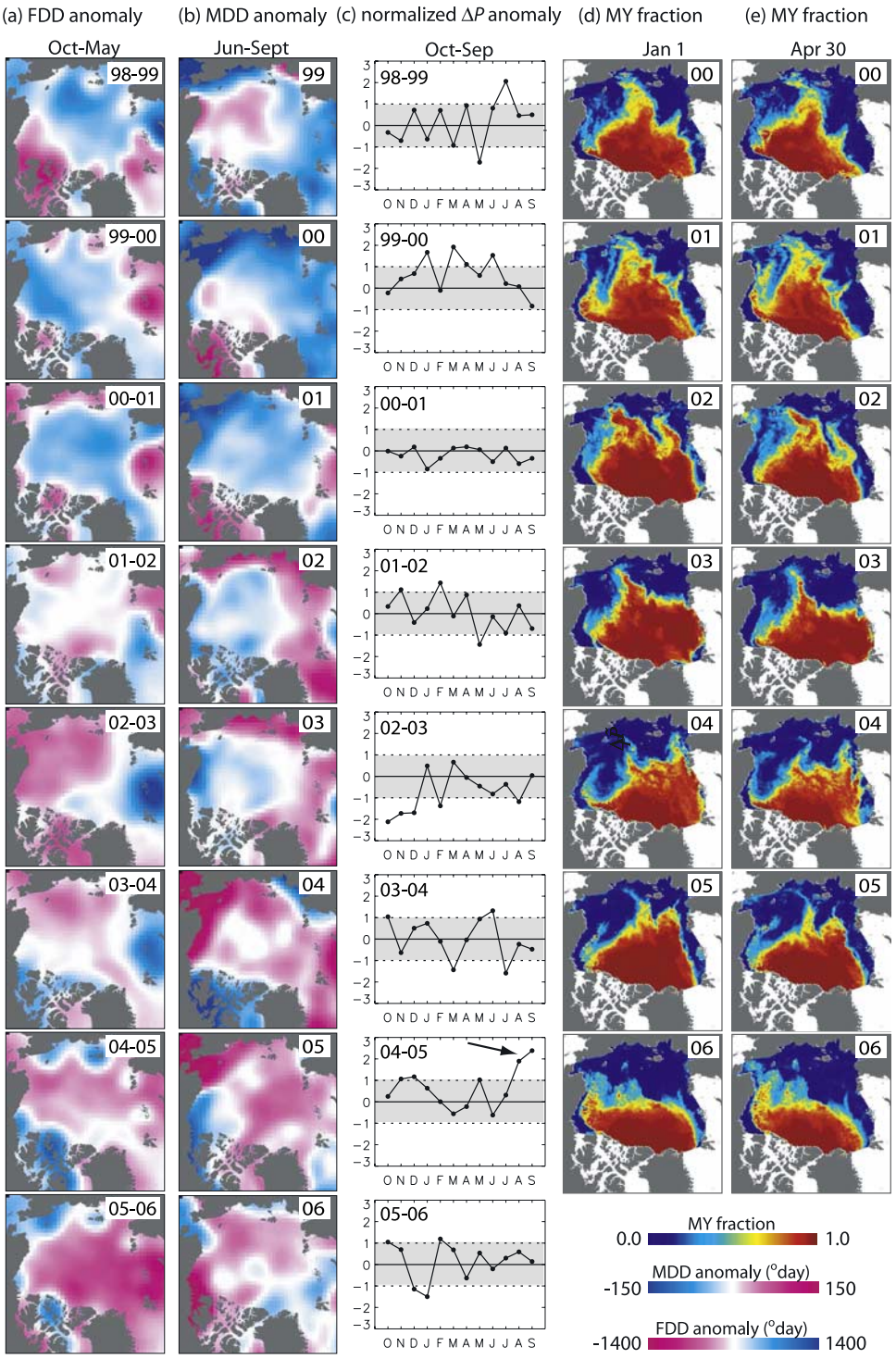

Figure 1. Winter multiyear ice coverage (2000–2006) and its relation to seasonal anomalies in freezing degree-days (F_{DD}), melting degree-days (M_{DD}), and normalized monthly anomalies in sea-level pressure gradient across the Fram Strait ($\Delta\tilde{P}$- see text for description) of the preceding season. (a) Oct–May F_{DD} anomalies, (b) Jun–Sep M_{DD} anomalies, (c) $\Delta\tilde{P}$, (d) MY coverage on January 1, and (e) MY coverage on April 30. Arrow points to the large deviations of $\Delta\tilde{P}$ from the mean in August and September of 2005.

have an opportunity to grow and thus a chance to survive the subsequent summer and contribute to the replenishment of the MY ice reservoir. This is not true of ice area exported during the summer; since there is no freezing of the vacated areas, summer export contributes directly to the depletion of the MY ice cover and open water production. Thus, from a replenishment perspective, for a given net annual ice export it would be better to have the higher ice export during the early winter than the summer. For the 2005 summer, ice export is directly responsible for ~40% of the ~0.6 × 10^6 km^2 of decrease in MY coverage. The warmer atmosphere and ocean explain the balance of this decrease.

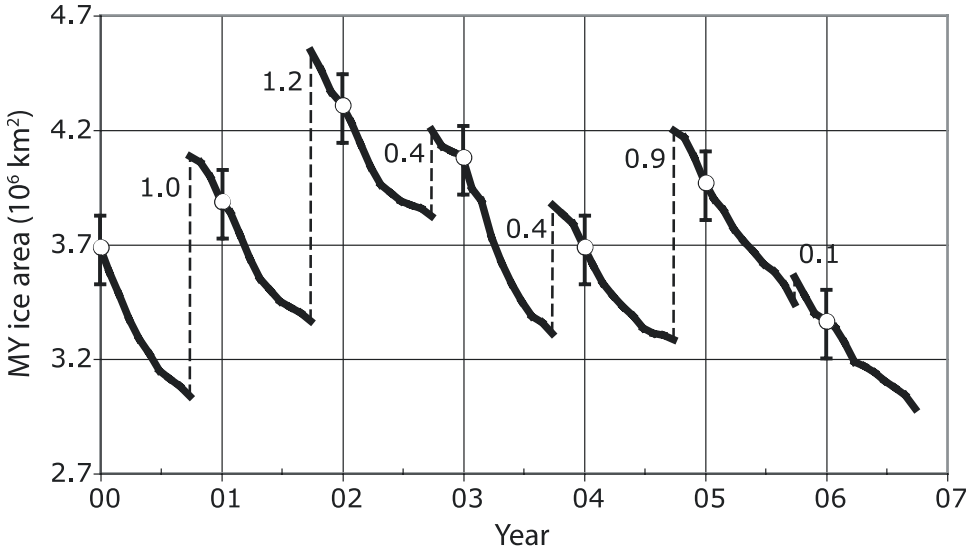

Figure 2. Seven annual cycles of Arctic Ocean multiyear ice coverage constructed using QuikSCAT data and ice export. The open circles show multiyear (MY) ice coverage on January 1. The dashed lines show the replenishment of the MY ice reservoir by first-year ice that survived the summer. The quantities next to the dashed lines are replenishment areas in 10^6 km^2.

3.3. Relationship to the Record of Freezing and Melting

[14] In this section, we examine the relationship between the record of A_r and the seasonal records of freezing and melting. The measures used here are the freezing degree-days (F_{DD}) between October and May and melting degree-days (M_{DD}) between June and September: F_{DD} is the cumulative sum of the daily mean temperatures below -1.8°C; and, M_{DD} is the cumulative sum of the daily mean temperatures above 0°C. Replenishment of MY ice at the end of each summer is clearly dependent on the M_{DD} of that summer but it also depends on the F_{DD} of the preceding winter as higher F_{DD}s indicate more growth, and thus a thicker ice cover that could survive the summer. Of course, the dependence on longer-term records of F_{DD} and M_{DD} is also important but their impact is more difficult to quantify and isolate because of the integrative nature of ice growth and melt.

[15] The first two columns of Figure 1 show the spatial fields of F_{DD} and M_{DD} anomalies of the seven years leading up to the summer of 2005 as well as that of the following winter and summer. The color scale is chosen such that cumulative temperatures indicating warmer seasons are in red, i.e., higher M_{DD} or reduced F_{DD}, and cooler seasons are in blue. On a broad Arctic Ocean scale, there is a negative trend in F_{DD} (less freezing) and a positive one in the M_{DD} anomalies (more melting temperatures). In fact, the winters and summers preceding the fall of 2005 have been anomalously warm – this is true even in the longer records of these parameters shown in Figure 4 (discussed below). Thus, the near zero replenishment of MY ice during the 2005 summer is potentially a cumulative effect of the persistent trends in F_{DD} and M_{DD} over this short record.

[16] One question that could be answered is whether there is any relationship between replenishment area, $\tilde{A}_r$ ('$\sim$' for anomalies), and the anomalies of the previous year's spatially averaged F_{DD} and the M_{DD} of the current summer (i.e., $\tilde{F}_{DD}$, $\tilde{M}_{DD}$). The spatial averages are taken over that area of the Arctic Ocean bounded by the passageways into the Pacific, and the Greenland and Barents Seas. To do this, we explore possible correlation between $\tilde{A}_r$ and the following variables: $\tilde{F}_{DD}$, $\tilde{M}_{DD}$, $\alpha\tilde{F}_{DD} + \beta\tilde{M}_{DD}$, and the correlation of the detrended $\tilde{A}_r$ with the same detrended variables. The sum of $\alpha\tilde{F}_{DD} + \beta\tilde{M}_{DD}$ is chosen to test whether the combination of variables better explains the variance. The results are: $\rho(\tilde{A}_r, \tilde{F}_{DD}) = 0.78, 0.56$; $\rho(\tilde{A}_r, \tilde{M}_{DD}) = -0.62, -0.01$; and, $\rho(\tilde{A}_r, \alpha\tilde{F}_{DD} + \beta\tilde{M}_{DD}) = 0.79, 0.62$. The first quantity is the correlation of the anomalies while the second is the correlation of the detrended anomalies. Because there are strong trends in each variable, the correlations are reduced after their removal. The previous winter's $\tilde{F}_{DD}$ explains more of the variance in $\tilde{A}_r$ than the detrended $\tilde{F}_{DD}$. This suggests, not surprisingly, that the replenishment area is dependent on the state (thickness and

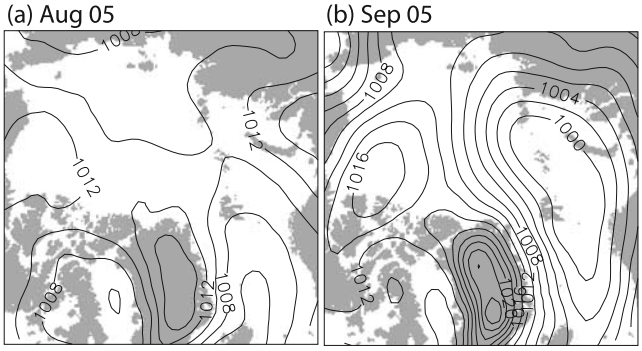

Figure 3. Mean sea-level pressure distributions in (a) August and (b) September of 2005. Contour interval is 2 hPa.

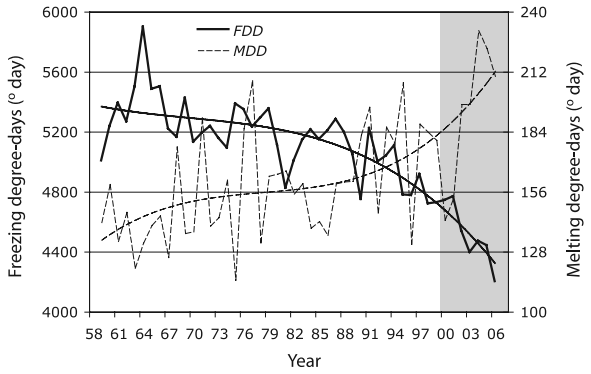

Figure 4. Time-series of spatially averaged F_{DD} and M_{DD} from 1958–2006. The spatial averages are taken over that area of the Arctic Ocean bounded by the passageways into the Pacific, and the Greenland and Barents Seas. For the F_{DD} time-series, the squared correlation increases from 0.64 to 0.76 from the linear to cubic fits (shown here). Similarly, for the M_{DD} the squared correlation increases from 0.26 to 0.32.

seasonal growth) of the ice cover entering the melt season. Similarly the summer's $\tilde{M}_{DD}$ explains more of the variance than the detrended $\tilde{M}_{DD}$. In fact, $\rho(\tilde{A}_r, \tilde{M}_{DD})$ is almost zero if $\tilde{M}_{DD}$ is detrended; this is most likely due to the fact that $\tilde{M}_{DD}$ is a much noisier variable since the air temperature is constrained to be near melting (i.e., ice bath) over most of ice cover during the summer. The much narrower range of variability of $\tilde{M}_{DD}$ compared to $\tilde{F}_{DD}$ can be seen in the degree-day scales in Figure 1. The linear combination of $\alpha\tilde{F}_{DD} + \beta\tilde{M}_{DD}$ explains ~63% and ~40% of the variance before and after detrending, and as expected is higher than those with the individual variables. With the caveat that only a short time-series is considered here, the results indicate that $\tilde{A}_r$ is correlated to the behavior of M_{DD} of the summer but more so to the F_{DD} of the preceding winter.

[17] It is also interesting to note that there seems to be little correlation between the spatial patterns of F_{DD} or M_{DD} anomalies (Figures 1a and 1b) and MY coverage of the following winter (Figure 1d). We expect that the changes in MY ice coverage associated with warming, unlike that of ice export which is immediate, to be a slower multi-year response and may not be attributable directly to the spatial warming effects of only the preceding summer and/or winter. This is in contrast to that of the behavior of the replenishment area.

[18] To place these eight recent years of F_{DD} and M_{DD} anomalies within the context of a longer-term multi-decadal record, we examine their spatially averaged behavior since 1958 (Figure 4). Again, the spatial averages are taken over that area of the Arctic Ocean bounded by the passageways into the Pacific, and the Greenland and Barents Seas. The gray region represents the extent of the short 8-year record shown in Figure 1. Linear and cubic polynomials are fitted to both time series (only cubic fits are shown in Figure 4). The F_{DD} time series shows clearly the accelerated warming since the mid-1980s; 80% of the net decrease in F_{DD} occurred after the mid-1980s. The positive trend in the M_{DD} is also clear, although the increasing slope in the cubic fit seems to be biased by the much higher M_{DD} of the last three years of the record. Nevertheless, both point to warmer winters and summers associated with what seems to be accelerating trends of warming over the Arctic Ocean during the past 20 years, and potentially lower average replenishment areas.

4. Conclusions

[19] The present note examines the end-of-summer replenishment of the multiyear ice cover using seven annual cycles of MY sea ice coverage derived from analysis of QuikSCAT observations and Arctic ice flux from satellite passive microwave data. To maintain a stable Arctic MY ice cover, the replenishment area at the end of summer must balance that area depleted by export and melt. The area available for replenishment of the MY ice cover relates directly to ice export, summer melt, and the thickness of the ice cover at the beginning of the melt season.

[20] The near zero replenishment of MY ice area at the end of the summer of 2005 (0.1×10^6 km^2) resulted in the lowest winter MY ice cover in the short record. The large depletion of the MY ice cover in the Eastern Arctic reported by *Nghiem et al.* [2006] is in part explained by the anomalous pressure patterns in August and September (Figure 3). During these months, a strong Trans-polar drift stream favoring source regions in the Eastern Arctic Ocean together with high ice flux through the Fram Strait removed a significant area of MY ice. These advective processes, typically significantly weaker during Arctic summers, created a large expanse of seasonal ice covering almost half the Arctic Ocean. For this summer, ice export is directly responsible for ~40% of the $\sim 0.6 \times 10^6$ km^2 decrease in MY coverage compared to January of 2005.

[21] For the short record examined here, the replenishment areas range up to 1.2×10^6 km^2 or ~20% of the Arctic Ocean (Figure 2). Variability is high. The highest MY coverage on this record follows two summers of relatively large replenishments. We also show that replenishment areas are correlated with the spatially averaged winter freezing degree-days (F_{DD}) and melting degree-days (M_{DD}) of the preceding winter (Oct–May) and summer (Jun–Sep). Both F_{DD} and M_{DD} are broad, cumulative measures of the seasonal near-surface air temperature histories. Positive correlation with the prior winter's F_{DD} suggests that the replenishment area is dependent on the state (thickness and seasonal growth history) of the ice cover entering the melt season. Warmer summers increase melt and result in negative correlation with M_{DD}. The linear combination of F_{DD} and M_{DD} explains ~63% of the variance, and as expected better explains the variance than the individual variables alone. Overall, the results suggest that a prior season's M_{DD} and F_{DD} are predictive of the survivability of the seasonal ice cover. The lower correlation between replenishment area and *MDD* means only that this parameter may not be the best measure of melt because of the limited range of variability of near surface summer air temperatures.

[22] Placing the trends of F_{DD} and M_{DD} of the past eight years within the context of a longer-term 48-year record, we find a gradual warming trend (Figure 4) of lower F_{DD} and higher M_{DD} during the first ~30 years which then accelerates after the mid-1980s. To date, the record does not shown any hint of recovery from these trends. If the correlations between replenishment area and F_{DD} and

M_{DD} hold over the longer term, then it is expected that the negative trend in MY ice coverage would continue. The impact of ice export is different during the winter and summer. In winter, seasonal ice produced in exported areas have an opportunity to thicken and thus have a chance to survive the summer and contribute to the replenishment of the MY ice cover of the following year. In contrast, large export episodes as experienced during the summer of 2005 would deplete the ice cover immediately and directly lead to increased absorption of solar radiation.

[23] From model simulations, *Lindsay and Zhang* [2005] report a thinning of the Arctic Ocean ice cover by ~1.3 m between 1988–2003. They hypothesized that the increased thinning rate during this period is likely due to the gradual warming of the Arctic over the last 50 years leading to reduced FY ice thickness at onset of melt, together with a short term increase in export of thick MY ice associated with changes in circulation patterns of the Arctic Oscillation in the late 1980s and early 1990s. The consequences are increases in the area of summer open water allowing increased heating of the ocean, creating a positive feedback scenario that favors additional thinning of the ice cover. From the perspective of replenishment area, our short record of observations certainly lend credence to their hypothesis: (1) the dependence of the replenishment area on F_{DD} of the preceding winter, i.e., the thickness of the FY ice entering summer; and (2) the impact of ice export – increased export requires a higher replenishment area for maintenance of the ice cover. Unfortunately, only a short record of replenishment areas is available here, but evidence seems to support that the replenishment areas (on the average) may no longer be sufficient to maintain a stable MY ice cover after the positive phase of the Arctic Oscillation, especially in the face of an accelerating warming trend and thinning of the Arctic sea ice.

[24] **Acknowledgments.** I wish to thank S. S. Pang for her assistance during the preparation of this manuscript. The SMMR and SSM/I brightness temperature and ice concentration fields are provided by World Data Center A for Glaciology/National Snow and Ice Data Center, University of Colorado, Boulder, CO. The QuikSCAT data were obtained from the Physical Oceanography Distributed Active Archive Center (PO.DAAC) at the NASA Jet Propulsion Laboratory, Pasadena, CA. This work was performed at the Jet Propulsion Laboratory, California Institute of Technology, under contract with the National Aeronautics and Space Administration.

References

Comiso, J. C. (2002), A rapidly declining perennial sea ice cover in the Arctic, *Geophys. Res. Lett.*, *29*(20), 1956, doi:10.1029/2002GL015650.

Comiso, J. C. (2006), Abrupt decline in the Arctic winter sea ice cover, *Geophys. Res. Lett.*, *33*, L18504, doi:10.1029/2006GL027341.

Johannessen, O. M., E. V. Shalina, and M. W. Miles (1999), Satellite evidence for an Arctic sea ice cover in transformation, *Science*, *286*(5446), 1937–1939.

Kalnay, E., et al. (1996), The NCEP/NCAR 40–year reanalysis project, *Bull. Am. Meteorol. Soc.*, *77*, 437–471.

Kwok, R. (2004), Annual cycles of multiyear sea ice coverage of the Arctic Ocean: 1999–2003, *J. Geophys. Res.*, *109*, C11004, doi:10.1029/2003JC002238.

Kwok, R., and D. A. Rothrock (1999), Variability of Fram Strait ice flux and North Atlantic Oscillation, *J. Geophys. Res.*, *104*, 5177–5190.

Kwok, R., G. F. Cunningham, and S. Yueh (1999), Area balance of the Arctic Ocean perennial ice zone: Oct 1996–April 1997, *J. Geophys. Res.*, *104*, 25,747–25,749.

Kwok, R., G. F. Cunningham, and S. S. Pang (2004), Fram Strait sea ice outflow, *J. Geophys. Res.*, *109*, C01009, doi:10.1029/2003JC001785.

Lindsay, R. W., and J. Zhang (2005), The thinning of Arctic sea ice, 1988–2003: Have we reached the tipping point?, *J. Clim.*, *18*, 4879–4895.

Nghiem, S. V., Y. Chao, G. Neumann, P. Li, D. K. Perovich, T. Street, and P. Clemente-Colón (2006), Depletion of perennial sea ice in the East Arctic Ocean, *Geophys. Res. Lett.*, *33*, L17501, doi:10.1029/2006GL027198.

R. Kwok, Jet Propulsion Laboratory, California Institute of Technology, 4800 Oak Grove Drive, Pasadena, CA 91109, USA. (ron.kwok@jpl.nasa.gov)